Desalination 479 (2020) 114326

Contents lists available at ScienceDirect

Desalination

journal homepage: www.elsevier.com/locate/desal

Feasibility study of reverse osmosis–flow capacitive deionization (RO-FCDI) for energy-efficient desalination using seawater as the flow-electrode aqueous electrolyte

Hyun Jun Chung, Jungbin Kim, David Inhyuk Kim, Gimun Gwak, Seungkwan Hong*

School of Civil, Environmental, and Architectural Engineering, Korea University, 145 Anam-ro, Seongbuk-gu, Seoul 02841, Republic of Korea

GRAPHICAL ABSTRACT

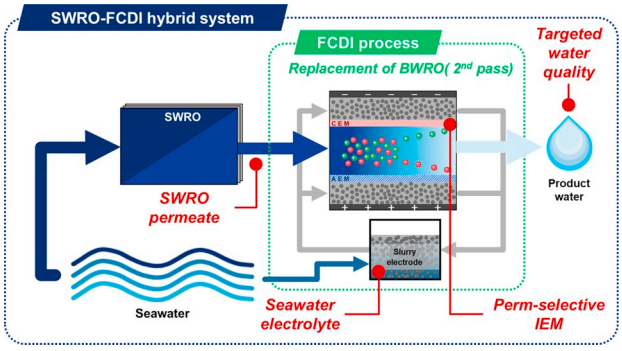

ARTICLE INFO

Keywords:
Flow electrode capacitive deionization (FCDI)
Seawater reverse osmosis (SWRO) desalination
Flow electrodes
Perm-selective ion exchange membrane (IEM)
Specific energy consumption (SEC)

ABSTRACT

Seawater reverse osmosis (SWRO) is usually combined with brackish reverse osmosis (BWRO) to improve the water quality in seawater desalination; however, this configuration often results in high energy consumption. Consequently, membrane capacitive deionization (MCDI) has been suggested as a lower energy alternative technology, but cyclic operation within the cell (i.e., discontinuous operation of ad/desorption) is a main disadvantage. On the other hand, flow electrode capacitive deionization (FCDI) can be continuously operated by using a flow electrode. In this study, the feasibility of a SWRO-FCDI system was examined by using a suitable electrolyte in the flow electrode: seawater or SWRO concentrate. In addition, by employing a selective ion exchange membrane (IEM), the FCDI was able to selectively remove monovalent ions rather than divalent ions, unlike BWRO, thus producing a final product water containing divalent ions, which is more suitable for corrosion control in the subsequent pipe distribution systems. As a result, the remineralization process can be minimized. To test the SWRO-FCDI concept, actual SWRO permeate was first treated in a single mode with an electrolyte comprising real seawater in a flow electrode, and the feasibility of long-term operation was proven by batch-mode, which allowed the optimization of the FCDI active area.

* Corresponding author.
E-mail address: skhong21@korea.ac.kr (S. Hong).

https://doi.org/10.1016/j.desal.2020.114326
Received 1 September 2019; Received in revised form 10 January 2020; Accepted 10 January 2020
Available online 24 January 2020

1. Introduction

Water scarcity is a severe challenge facing the 21st century. Further, the production of safe drinking water from various water resources is becoming more complicated because of climate change, as well as the contamination of water resources resulting from industrialization and urbanization. One way to produce clean drinking water is to use a desalination process to treat saline water. Among the available technologies, seawater reverse osmosis (SWRO) technology has been widely used for seawater desalination [1,2]. Two main advances in SWRO technology have been made in the past three decades [3]. First, the development of thin-film composites SWRO membranes, which enables high salt rejection and high water permeability [2,4], and second, the coupling of energy recovery devices, which reduces overall energy consumption of SWRO systems [1,2,5]. These technical innovations have made SWRO processes sustainable options for meeting freshwater demand [6].

In the early stages of SWRO application, an RO system is configured as a single stage; this recovers 40–50% of the feed water as the permeate [1,2,7,8]. The salinity of the SWRO permeate is affected by various factors, including the feed salinity and the membranes in use, but it generally has a total dissolved solids (TDS) < 500 mg/L. However, the quality of the SWRO permeate requires further improvement (i.e., salinity reduction) when it is to be utilized for certain purposes such as agricultural use, industrial use, or drinking water. This can be achieved by utilizing brackish water reverse osmosis (BWRO), which can reduce the TDS of SWRO permeate further to meet these requirements [7]. In the BWRO system, the RO system first carries out SWRO on seawater and then carries out BWRO on the brackish water produced from the first stage; thus, it is denoted a two-pass system. Recent SWRO plants have adopted the two-pass RO system to produce purer permeates [1,7].

Recently, the application of membrane capacitive deionization (MCDI) has been investigated in academia [9–12]. For example, for the treatment of brackish water, a new electrochemical double-layer capacitor using active carbon and multi-walled carbon nanotubes has been investigated [10]. In addition, brackish water containing oily compounds has been treated with activated carbon granules as a cost-effective electrode material that improves the electro-sorption efficiency [11]. In addition, MCDI has been used as a BWRO alternative in the development of a system for bromide removal and reverse electrodialysis [9,12]. These attempts to use the MCDI process for the BWRO process suggest a means to reduce energy consumption compared to the standard BWRO processes. However, the MCDI process is based on solid-state electrodes whose surfaces easily become saturated with ions, thus necessitating the cyclic operation of the cell, i.e., adsorption and desorption. In contrast, a newly developed desalination technology, flow electrode capacitive deionization (FCDI), allows the continuous supply of the uncharged flow electrode by replacing the solid electrode [13,14]. In addition, the introduction of an FCDI flow electrode enables the transfer of ions between the feed and the flow electrode without energy consumption due to the ion concentration gradient.

Recent studies of FCDI concerning the flow electrode have focused on improving performance by changing the carbon content or the electrolyte. For example, a higher carbon weight ratio in the flow electrode results in the removal of more salts; however, the electrode viscosity increases, which can result in clogging. To increase the carbon weight ratio, the use of activated carbon (AC) having a surface modified with a polymer layer coating has been tested, and up to 35 wt% carbon loading has been achieved without clogging [15]. Another way of enhancing the AC loading is to use the gravity and large AC particles [16]. Meanwhile, for the electrolyte, a high salt concentration and the addition of additives such as carbon nanotubes, carbon black, and redox-active species facilitate charge transfer, resulting in an increase in the desalination efficiency [14,17–20].

Table 1
Comparison of CDI-related experimental objectives and experimental conditions.

Feed solution	Aqueous electrolyte in flow electrode	Flow electrode pretreatment methods	Assessment of energy consumption	Selectivity of divalent ions	Process development objective	Reference
NaCl, $CaCl_2$, $MgCl_2$, SWRO permeate	NaCl, seawater (i.e., SWRO feed)	Sonication	Yes	Yes	Feasibility of SWRO-FCDI process (first suggestion)	This paper
NaCl	NaCl	N/A	N/A	N/A	Achievement of high recovery of ammonia solution	[21]
NaCl	NaCl	N/A	N/A	N/A	Production of dilute and concentrate streams in a single cell	[22]
NaCl, $MgSO_4$	NaCl	N/A	N/A	Yes	Combination of NF membrane in FCDI cell	[23]
NaCl	NaCl	Sonication	Yes	N/A	Feasibility of energy efficient FCDI-NF process	[24]
NaCl, $CaCl_2$	NaCl	N/A	Yes	Yes	Softening brackish water	[25]

MEA: Monoethanolamine (MEA was employed for energy harvesting because of the higher solubility of CO_2 compared to pure water).

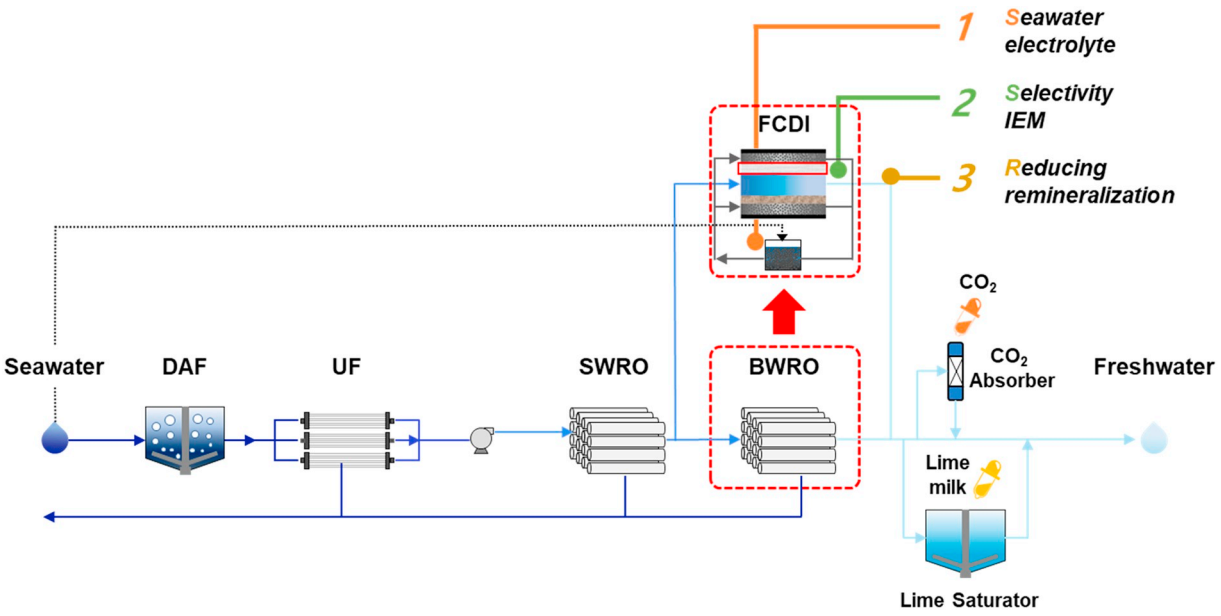

Fig. 1. Schematic of SWRO-FCDI hybrid system. The lower part in the above figure is the SWRO-BWRO process diagram. The red dotted line represents the replacement of the existing BWRO process with the FCDI process. DAF: dissolved air flotation, UF: Ultrafiltration. (For interpretation of the references to colour in this figure legend, the reader is referred to the web version of this article.)

However, of the studies involving FCDI, there has been little investigation into the effect of the source water in the feed water and the electrolyte in the flow electrode. Further, most studies have focused on improving the process performance without considering the energy consumption. Concerning FCDI applications, studies have investigated the use of flow electrodes to enhance the recovery of ammonia from solution [21]. In addition, the use of a nanofiltration (NF) membrane with an anion exchange membrane (AEM) and cation exchange membrane (CEM) has been used for continuous operation in a single cell for the simultaneous treatment of permeate and concentrate [22]. Additionally, an NF membrane with an exchange membrane having selectivity for divalent ions, especially anions (i.e. sulfate ions), has been introduced [23]. Another process was developed using a hybridized NF system for the post-treatment of FCDI, resulting in a process comparable to BWRO [24]. Furthermore, a method for treating brackish water with a water softening process has been proposed [25] (Table 1). Lastly, it should be noted that there have been no investigations of the use of FCDI for seawater desalination using real feed water and electrolyte in the flow electrode.

In this study, the feasibility of a new SWRO-FCDI hybrid system (Fig. 1) was first investigated. One of the advantages of using the SWRO-FCDI process is that it consumes less energy while showing similar performance to the existing SWRO-BWRO process. To prove these advantages, we analyzed the ion removal efficiency and energy consumption when using simulated seawater and SWRO concentrate as the electrolyte in the flow electrode; the utilization of such water sources as electrolyte is an important advantage of FCDI. Additionally, in the traditional SWRO-BWRO process, the treated water is highly corrosive, so post-treatment is required [26]. When using a selective ion exchange membrane (IEM), the ratio of divalent ions in the treated water of the FCDI process can be increased, thereby reducing the burden of the post remineralization process. Furthermore, to verify the feasibility of the SWRO-FCDI system under realistic conditions, actual SWRO permeate and a real seawater electrolyte in the flow electrode were employed in batch mode, and these laboratory-scale experiments were used to determine the FCDI active area that achieves the optimal performance.

2. Materials & methods

2.1. Feed solution

A NaCl feed solution was used to investigate the basic performance of the FCDI process. Its feed concentration was determined as 500 mg/L in TDS, and this represents the SWRO permeate in our study. To explore the selectivity of FCDI for divalent ions, solutions containing $MgCl_2$ and $CaCl_2$ at 500 mg/L in TDS were also examined. Each species, such as NaCl (Junsei Chemical Co., Japan), $MgCl_2$ (Sigma–Aldrich Co., USA), and $CaCl_2$ (Sigma–Aldrich Co., USA), was dissolved in ultrapure deionized (DI) water. The feasibility of the SWRO-FCDI hybrid process was also evaluated by using real SWRO permeate from a pilot plant. The SWRO pilot plant in Yeosu, Republic of Korea, produces 25 m^3/d of treated water (Fig. 2). However, because the concentration of permeate is 500 mg/L (Table 2), it requires further treatment for TDS reduction.

2.2. Flow electrodes

2.2.1. Electrolyte

To select a suitable electrolyte concentration for the flow electrode for the SWRO-FCDI process, experiments with the flow electrode were conducted with three different NaCl concentrations (e.g., 500, 35,000, and 66,000 mg/L), simulating SWRO permeate, seawater, and SWRO concentrate, respectively. To analyze the effect of the divalent ions, a flow electrolyte containing 35,000 mg/L NaCl was employed. However, when the feasibility of the SWRO-FCDI process was examined, real seawater was utilized.

2.2.2. Activated carbon

In the preparation of the flow electrode, in all experiments, activated carbon (P60, Kuraray co., Japan) was added at the same weight percentage, i.e., 60 g in 400 mL ultrapure deionized (DI) water (13.04 wt%). The morphology of the AC particles was observed by scanning electron microscopy (SEM, S-4800, HITACHI Ltd., Japan) and confirmed to be spherical. The average size of the activated carbon was analyzed using the Japanese Industrial Standard (JIS K 1474) method, and the values are listed in Table 3. The specific surface area, average pore diameter, and total pore volume of the P-60 activated carbon were

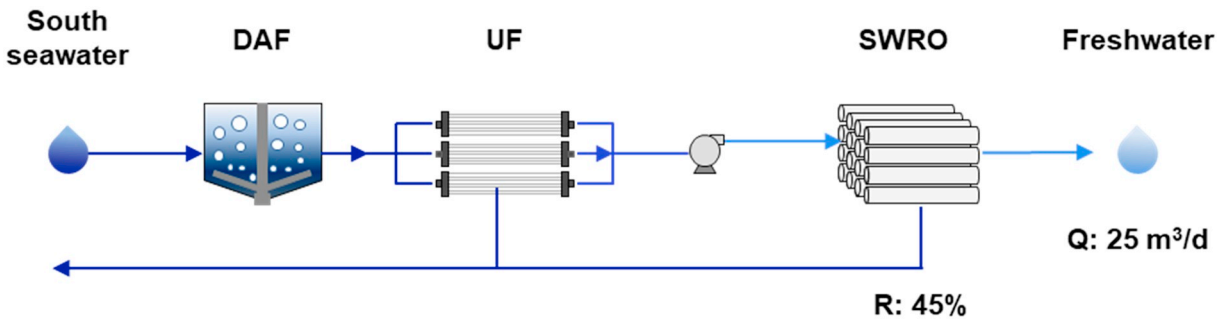

Fig. 2. Schematic of the RO pilot plant in Yeosu, Republic of Korea. The detailed specification of the process is confidential. R: recovery, Q: flow rate.

Table 2
Composition and concentration of the real SWRO permeate and seawater.

Composition	SWRO permeate (mg/L)	Seawater (mg/L)
Na^+	161.8 ± 1.8	9516.0
K^+	8.49 ± 0.9	390.2
Ca^{2+}	2.7 ± 1.1	413.4
Mg^{2+}	5.9 ± 0.6	1294.1
Cl^-	222.3 ± 26.1	11,665.3
SO_4^{2-}	22.15 ± 17.6	2024.8
TDS	548.68 ± 125.3	33,776

Table 3
Activated carbon (P-60) particle size distribution before and after sonication.

	Before sonication	After sonication
Size distribution	< 45 μm (91.8%) (JIS K 1474)	< 31.01 μm (90%) (ISO 13320)

found to be 1354.8 m^2/g, 1.95 nm, and 0.66 cm^3/g, respectively, which were analyzed by the Brunauer–Emmett–Teller (BET) method (BELSORP-MAX, BEL Japan Co., Japan). To achieve a homogeneous carbon suspension, the flow electrode was stirred for 24 h using a magnetic stirrer bar. In addition, the flow electrode was sonicated to improve the FCDI performance by changing the morphology of the AC particles. After 240 min of sonication, the BET surface area of the activated carbon was increased from 1354.8 to 1584.7 m^2/g (16.97% increase). As shown in Fig. 3, sonication (model 350, Branson Sonic Power Co, Danbury, CT) played an important part in the formation of the spherical morphology and the reduced diameter of the activated carbon particles.

2.3. Lab-scale FCDI cell

In Fig. 4, the assembly of the FCDI cell is illustrated. The cell consists of a pair of graphite current collectors with CEM, AEM, a gasket, a spacer, and end plates. The geometry of the graphite current collector is 2 mm (width), 74 mm (length), and 2 mm (height). The active area between the IEM and flow electrode is 36.3 cm^2.

2.4. Operation of the FCDI cell

The feed flow rate through the spacer was set to be 5 mL/min and that through the flow electrode was set to 30 mL/min in all experiments. The FCDI cell was operated in the single mode to investigate the feasibility of using the flow electrode with simulated seawater and SWRO concentrate and to monitor the effect of the divalent ions in the feed with a perm-selective IEM. In contrast, both single and batch modes were used to examine the feasibility of using actual SWRO permeate as the feed and real seawater as the flow electrolyte (Table 4). In both single and batch modes, a short-circuited closed cycle (SCC) with a mixed flow electrode as the anode and cathode was used. Constant voltages of 0.00, 0.25, 0.50, 0.75, and 1.00 V were applied to the FCDI cell using a potentiostat (ZIVE SP5, Wonatech, Republic of Korea) to investigate the feasibility of using seawater in the flow electrode. The batch-mode experiments described in Section 3.4 were conducted at a constant voltage of 0.50 V for the purpose of optimizing the hydraulic retention time (HRT), considering the difficulty of single pass experiments in lab-scale long-term operation. The conductivity was measured with a conductivity meter (Hach, CDC401). Each experiment was conducted for 30 min except for the long-term batch-mode experiments. In addition, the experiment was run at least three times to increase the reliability of the experiment.

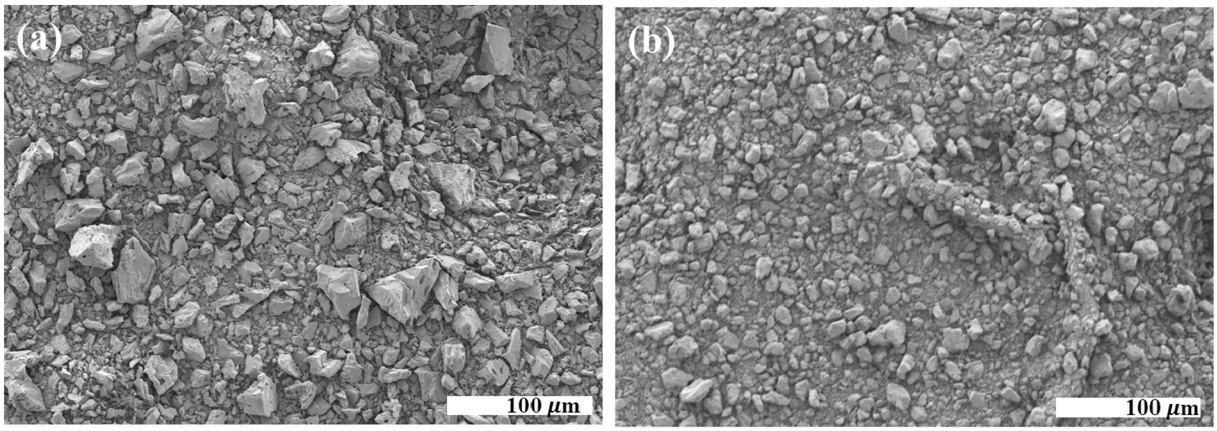

Fig. 3. Morphology of activated carbon (P-60) (a) before sonication and (b) after 240 min of sonication.

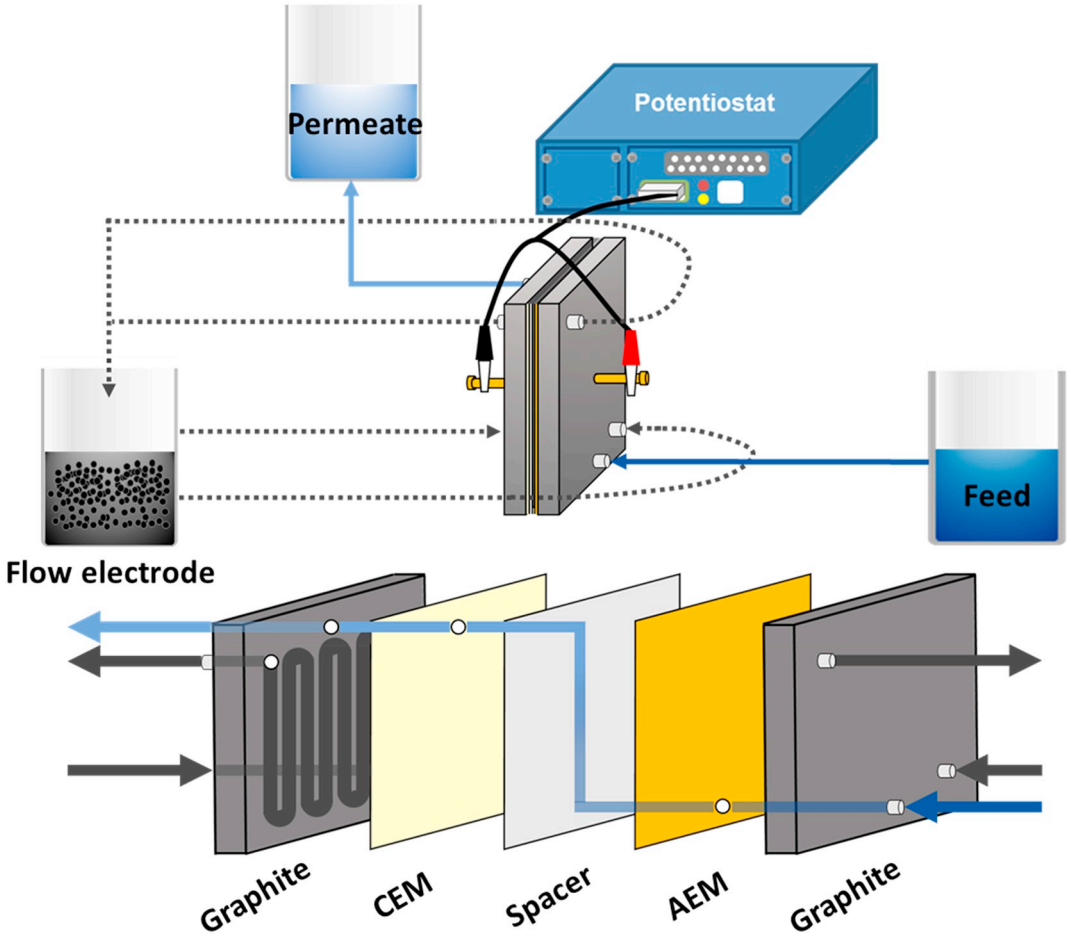

Fig. 4. Diagram of the FCDI cell containing graphite anode and cathode, cation exchange membrane (CEM), anion exchange membrane (AEM), spacer between ion exchange membrane, and end plates made of polyvinyl chloride (PVC) at both ends.

Table 4
Feed solution components and concentrations.

Section	(a) Feed solution	(b) Electrolyte
3.1	NaCl 500 mg/L in TDS	NaCl 500 mg/L in TDS NaCl 35,000 mg/L in TDS NaCl 66,000 mg/L in TDS
3.2	NaCl 500 mg/L in TDS $MgCl_2$ 500 mg/L in TDS $CaCl_2$ 500 mg/L in TDS	NaCl 35,000 mg/L in TDS
3.3, 3.4	SWRO permeate	Seawater

2.5. Analysis of FCDI performance and energy assessment

To enable performance analysis and comparison of the FCDI system, performance and efficiency indicators are required; these can be expressed by the removal efficiency, energy consumption, energy efficiency, specific energy consumption (SEC), salt adsorption capacity (SAC), and average salt adsorption rate (ASAR). The FCDI performance is determined by how much and how quickly the ions are removed from the feed water, i.e., the SAC, indicating the amount of desalination achieved during the charging process, and the ASAR, respectively. The removal efficiency (%) was calculated using Eq. (1), where C_i and C_f are the initial feed and final effluent concentrations (mg/L in TDS), respectively. Eq. (2) was used to calculate the energy consumption of FCDI in joules, where t is the operating time, E is the applied potential, and I is the current. In Eq. (3), the energy efficiency (%) is used to represent the total energy consumption per unit amount of removed ions. The SEC (kWh/m^3) was calculated using Eq. (4), where t is operating time, E is the applied potential, I is current, and V is the permeate volume (m^3). Eq. (5) is the salt adsorption capacity, SAC (mg/g), which represents the CDI cell performance where Q is the flow rate (mL/min) and "*AC weight*" is the weight of dried AC used in the flow electrode. The average salt adsorption rate, which is considered as one of the actual electrode properties, ASAR (mg/(g min)) was calculated with Eq. (6), where *SAC* is obtained from Eq. (5).

$$\text{Removal Efficiency (\%)} = \frac{C_i - C_f}{C_i} \times 100 \quad (1)$$

$$\text{Energy Consumption (J)} = \int_0^t \text{EI(t)dt} \quad (2)$$

$$\text{Energy Efficiency (kJ/mol)} = \frac{Enrgy\ consumption\ (kJ)}{Removed\ ions\ (mol)} \quad (3)$$

$$\text{Specific Energy Consumption (kWh/m}^3\text{)} = \frac{E\int Idt}{V} \quad (4)$$

$$\text{Salt Adsorption Capacity (mg/g)} = \frac{\int (C_i - C_f)Qdt}{AC\ weight} \quad (5)$$

$$\text{Salt Adsorption Rate } (mg/g/min) = \frac{SAC}{time} \quad (6)$$

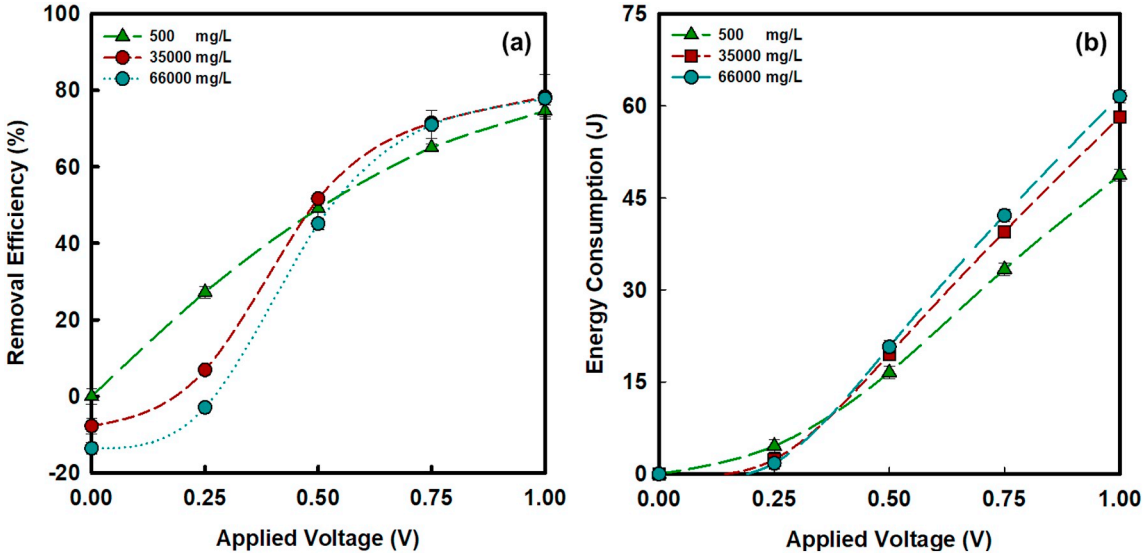

Fig. 5. FCDI performance with various electrolytes in the flow electrode using NaCl solutions having concentrations approximating those of SWRO permeate, seawater, and SWRO concentrate in single mode for 30-min operation in stepped increases of 0.25 V from 0.00 to 1.00 V: (a) removal efficiency (%) and (b) energy consumption (J).

3. Results and discussion

3.1. Evaluation of simulated SWRO concentrate as an FCDI electrolyte

In the SWRO-FCDI system, the electrolyte source should be easily available near the SWRO system to enable constant FCDI operation. Thus, the abundant and available water streams in the SWRO plants, such as seawater and SWRO concentrate, can be utilized as the electrolyte. However, the concentration difference between the feed and the electrolyte results in an ion concentration gradient, and, accordingly, the feed concentration increases. Thus, the concentration of the electrolyte should be carefully determined when treating low-concentration feeds [20,27].

When the electrolyte contained a higher TDS concentration than the FCDI feed, better removal efficiency was achieved at voltages higher than 0.5 V (Fig. 5a). At 0.75 V, 63.06% removal efficiency was achieved using the electrolyte with a TDS of 500 mg/L (i.e., the same concentration as the feed), whereas the electrolytes having TDS values of 35,000 and 66,000 mg/L showed higher removal efficiencies of 70.23% and 68.82%, respectively. Similarly, better performance was observed at 1.00 V when using the electrolytes with high TDS concentrations. This is because the surface charge density in the electrical double layer (EDL) is increased when the concentration of the electrolyte is elevated (e.g., the use of 35,000 and 66,000 mg/L TDS compared to 500 mg/L TDS), resulting in higher performance [28]. On the other hand, a negative removal efficiency was obtained in the cases where no or low voltage was applied to the FCDI system [29].

Although the electrolytes with higher TDS concentrations exhibited better removal efficiencies at high voltages, the energy consumption was also elevated (Fig. 5b). When the 500 mg/L electrolyte was employed, the FCDI system consumed 0.03–0.09 J in the range of 0.50–1.00 V. On the other hand, for electrolytes containing 35,000 and 66,000 mg/L TDS, only 0.03–0.1 and 0.03–0.11 J, respectively, were required to operate the FCDI system. Because these values depend on the electrolyte concentration, the energy efficiency (i.e., energy used to remove one mole of salt; kJ/mol) was also evaluated. We found that 0.50 V was the most energy efficient voltage in all cases, yielding 26.7, 29.9, and 35.7 kJ/mol for electrolyte concentrations of 500, 35,000, and 66,000 mg/L, respectively.

When considering use in actual plants, the use of SWRO permeate as an electrolyte in the flow electrode reduces the recovery rate, whereas the removal efficiency was improved when using the simulated seawater and SWRO concentrate. Consequently, in terms of removal efficiency, energy consumption, and energy efficiency, it is reasonable to select an electrolyte concentration similar to that of seawater rather than that of the SWRO concentrate for use as the flow electrode in the SWRO-FCDI system.

3.2. Retention of divalent ions for hardness control

The water produced from the BWRO process requires post-treatment for remineralization before water distribution because of its low mineral content, hardness, alkalinity, and pH [26,30]. Accordingly, most seawater desalination plants add chemicals during post-treatment, mainly lime, to increase the calcium ion concentration [31]. However, it has been reported that the use of a perm-selective IEM in CDI-like processes can remove monovalent ions better than divalent ions [32]. If the FCDI process can also exhibit a lower removal efficiency, particularly for divalent ions, the hardness of the produced water can be improved compared to that of the BWRO process. Because the removal tendency of mono- and divalent ions has not been investigated, we conducted experiments using solutions containing mono- and divalent ions (particularly cations).

When a voltage was applied to the FCDI cell, we found that the removal efficiency for monovalent ions was greater than that for divalent ions. As shown in Fig. 6a, the reverse flux of the divalent ions occurred regardless of the type of ions in the feed (i.e., mono- or divalent) when no voltage was applied. Starting from 0.25 V, it was observed that ions in the feed overcame the concentration difference in the feed and the electrolyte. In general, the monovalent ions showed better rejection than the divalent ions. The highest removal efficiencies for NaCl, $MgCl_2$, and $CaCl_2$ were 76.72%, 37.98%, and 56.06%, respectively, at 1.00 V, but the greatest differences between the removal efficiencies of the monovalent and divalent ions were 50.46%, 14.29%, and 19.19% at 0.50 V, respectively. The ion perm-selectivity behaved differently depending on the charge and ion radius. It can be inferred that Mg^{2+} (ionic radius = 0.078 nm) would be removed to a greater extent than to Ca^{2+} (ionic radius = 0.106 nm) because of its larger ion radius. However, because the hydrated ion of Mg^{2+} (0.395 nm) is larger than that of Ca^{2+} (0.348 nm) [33], the removal efficiency of $CaCl_2$ was higher than that of $MgCl_2$. Thus, the hydrated ion radius should be considered for the selective removal of ions [34,35].

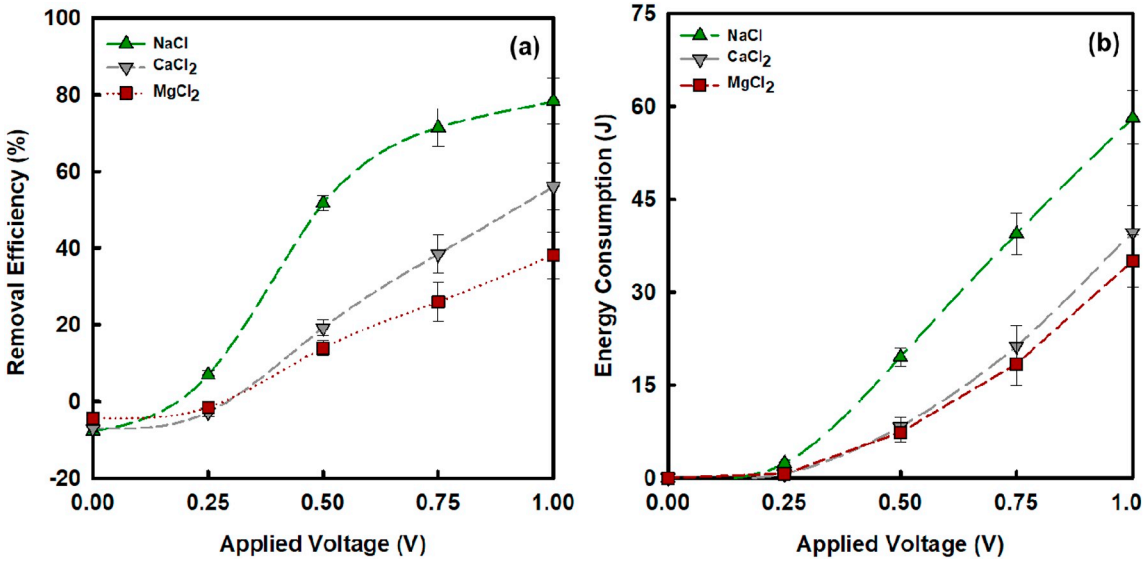

Fig. 6. FCDI performance with NaCl, $MgCl_2$, and $CaCl_2$ feed water and 35,000 mg/L NaCl flow electrode representing seawater with 30-min operation with 0.25-V step increases from 0.00 to 1.00 V with respect to the (a) removal efficiency (%) and (b) energy consumption (J).

As shown in Fig. 6b, energy was consumed in increasing order of NaCl, $CaCl_2$, and $MgCl_2$. When the difference in the removal efficiency was the highest at 0.50 V, the energy consumption values were 19.5, 8.2, and 7.3 J for NaCl, $MgCl_2$, and $CaCl_2$, respectively. However, the energy efficiency decreased in the order of NaCl, $CaCl_2$, and $MgCl_2$, i.e., 29.9, 56.0, and 56.8 kJ/mol, respectively, which means that more energy is consumed when the divalent ions are removed from the feed. As a result, the experiments using a NaCl solution consume more energy than those using the mixed solution, that is, the real SWRO permeate feed water.

The FCDI system can remove both monovalent and divalent ions with different removal efficiencies when using a perm-selective IEM. In the current two-pass SWRO system composed of a SWRO–BWRO pair, a remineralization process is required to supplement depleted divalent cations such as Ca^{2+} to prevent pipe corrosion in the water distribution system [32], which further increases energy consumption and operating costs. However, SWRO-FCDI can be used to produce water with a higher divalent ion concentration than that produced by the SWRO-BWRO system, thus reducing the need for remineralization treatment.

3.3. Performance of the SWRO-FCDI system

Using performance tests, the feasibility of the SWRO-FCDI system was examined by treating actual SWRO permeate. The SWRO permeate was obtained from a pilot plant in Yeosu (Fig. 2). Because the TDS of this permeate is higher than those of typical SWRO plants, the SWRO permeate was treated by the FCDI system to reduce the effluent TDS concentration to 200–300 mg/L [7,8]. As the flow electrode electrolyte, real seawater was used in consideration of the practical application of the system. The SWRO-FCDI performance was evaluated in terms of effluent TDS, removal efficiency, SAC, and SEC at voltages from 0.00 to 1.00 V.

The FCDI system can reach a TDS of < 300 mg/L at voltages > 0.5 V at an HRT of 0.98 min. The results from single mode operation with a SCC are presented in Fig. 7a. When applying 0.00 V to the FCDI cell, the effluent concentration was 661.0 mg/L in TDS because of the ion gradient resulting from the ion concentration difference between the SWRO permeate and seawater electrolyte. An effluent TDS of < 300 mg/L was achieved by increasing the voltage above 0.50 V, and the lowest obtained effluent TDS was 150 mg/L at an applied voltage of 1.00 V. The results imply that treating SWRO permeate with a seawater flow electrode is effective for lowering the TDS concentration. However, the HRT of the laboratory scale FCDI was very low, 0.98 min, which suggests that the effluent concentration can be further lowered if the HRT is increased.

The combined SWRO–FCDI system also acts as a low-energy desalination process. The range of voltages that overcome the concentration difference between the feed and flow electrode was 0.00–0.25 V, and the SEC was below 0.005 kWh/m^3 (Fig. 7b). The application of 0.50 V resulted in an increase in the SEC to 0.03 kWh/m^3, but the resultant effluent TDS was below 300 mg/L. An effluent concentration of 150 mg/L was obtained at the highest applied voltage (1.00 V), having a SEC of 0.09 kWh/m^3. Although the SEC of the FCDI system is lower than that of the BWRO system [36], the permeate quality would be inferior to that of BWRO. Thus, the performance of FCDI should be further assessed using identical FCDI and BWRO test conditions.

However, the performance of the FCDI system can be improved further because the SAC is not at equilibrium. The SAC value indicates how much salt is removed during the adsorption step in the FCDI process [37–39]. The SAC is presented with respect to the weight of AC in single mode SCC, and the SAC increased with operating time (Fig. 8a). In particular, SAC values of 0.11, 0.63, 0.90, and 1.13 mg/g were obtained when applying voltages of 0.25, 0.50, 0.75, and 1.00 V, respectively. In fact, the SAC values were lower than those from other studies, which resulted from the low feed concentration (i.e., SWRO permeate) [40]. However, the FCDI process did not reach an equilibrium state in the applied voltage range of 0.00–1.00 V. Thus, the AC can further absorb ions until the maximum SAC (mSAC) if the HRT is increased [41].

The ASAR of the FCDI was mainly affected by the voltage potential, and the ASAR took longer to reach equilibrium at higher voltages. The SAR is another important metric to describe the cell performance, which is a combination of cell architecture, charging time, electrode materials, and AC kinetics [29]. In Fig. 8b, the SAR results show that the FCDI performance reached equilibrium at different times depending on the applied voltage. The SAR in equilibrium was 0.004, 0.021, 0.03, and 0.039 mg/(g min) for 0.25, 0.50, 0.75, and 1.00 V, respectively. The ASAR values of the FCDI system are similar to those (ASAR = 0.025 mg/(g min)) from another study where the experimental AC loading was 11.11 wt% AC and the voltage was 1.2 V [41]. Overall, the SWRO-FCDI system utilizing seawater electrolyte was able to produce water with a TDS of < 300 mg/L.

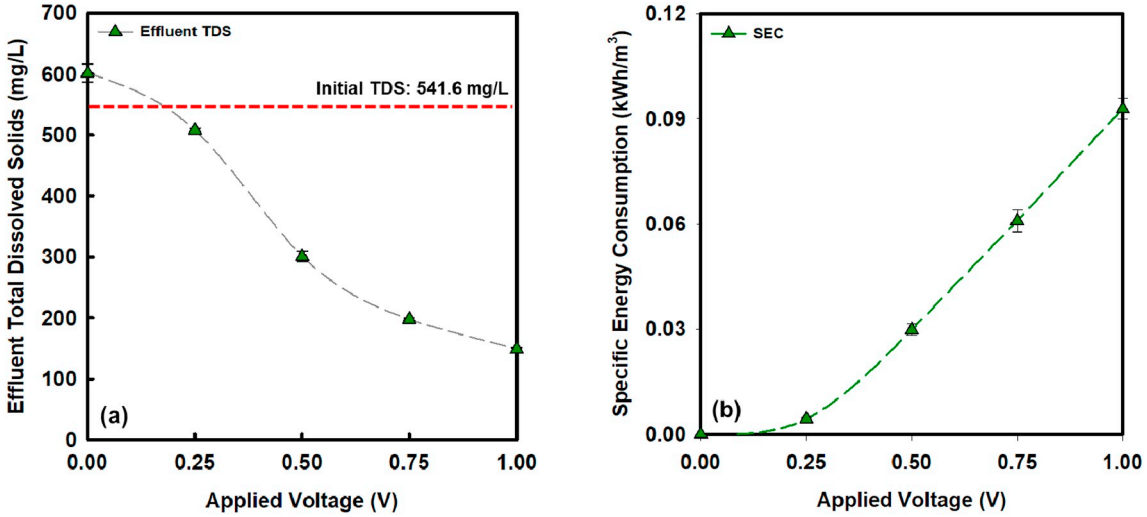

Fig. 7. FCDI performance with SWRO permeate feed water and a seawater flow electrode in single mode on increasing the voltage in 0.25-V steps from 0.00 to 1.00 V with respect to (a) effluent total dissolved solids (mg/L) and (b) SEC (kWh/m^3). The red dotted line refers to the initial TDS of SWRO permeate. (For interpretation of the references to colour in this figure legend, the reader is referred to the web version of this article.)

3.4. Scaling-up the SWRO-FCDI system

To evaluate the FCDI performance at equilibrium, the FCDI must be operated with a longer HRT. A batch-mode FCDI system can simulate a series of FCDI systems (i.e., FCDI system with longer HRT) and allow the evaluation of the optimal FCDI process. This means the best performance of the FCDI system can be obtained from batch-mode experiments, thus allowing comparison with the BWRO system and revealing the feasibility of the SWRO-FCDI process compared to that of SWRO-BWRO. Thus, the FCDI system was operated for 120 h at 0.50 V, which was the most energy-efficient condition for obtaining the 300 mg/L TDS observed in previous experiments.

The removal rate of the long-term operation FCDI system was comparable or even higher to that of the BWRO system [42]. As shown in Fig. 9a, the effluent TDS according to operating time (extended HRT) is illustrated, and the effluent TDS was reduced from 28.3 to 12.2 mg/L during operation from 30 to 120 h. At an HRT of 12 h, the effluent TDS was 108.4 mg/L, whereas, at an HRT of 21 h, a TDS of 49.3 mg/L was achieved. In single mode, the active area of the FCDI is fixed, and, thus, the achievable water quality of the effluent is limited. However, a larger active area can be assumed when operating FCDI in batch mode, and a target effluent concentration of 12 mg/L TDS was achieved after 120-h operation. Consequently, SWRO-FCDI systems can compete with SWRO-BWRO systems in terms of water quality.

Moreover, the FCDI system exhibited even lower energy consumption compared with the BWRO system when operated for 120 h. The FCDI system consumed 1.3 kWh/m^3 to achieve an effluent concentration of 12.2 mg/L (Fig. 9a and b). On the other hand, approximately 0.3 kWh/m^3 of energy was consumed in lab-scale to lower the TDS from above 200 mg/L to nearly 100 mg/L. Considering the range of BWRO energy consumption is 0.2–0.4 kWh/m^3 [1,7], SWRO-FCDI would be more energy efficiency over SWRO-BWRO at real scale with the improvement in pump efficiency at larger capacity. Given the operating time, which can be assumed to be equal to the HRT, the corresponding active area required to achieve the target effluent TDS in real single mode operation can be calculated. For example, if the wastewater concentration is < 20 TDS, the HRT is 40 h and the active area at that time is 8.7 m^2. Consequently, if sufficient active membrane area is

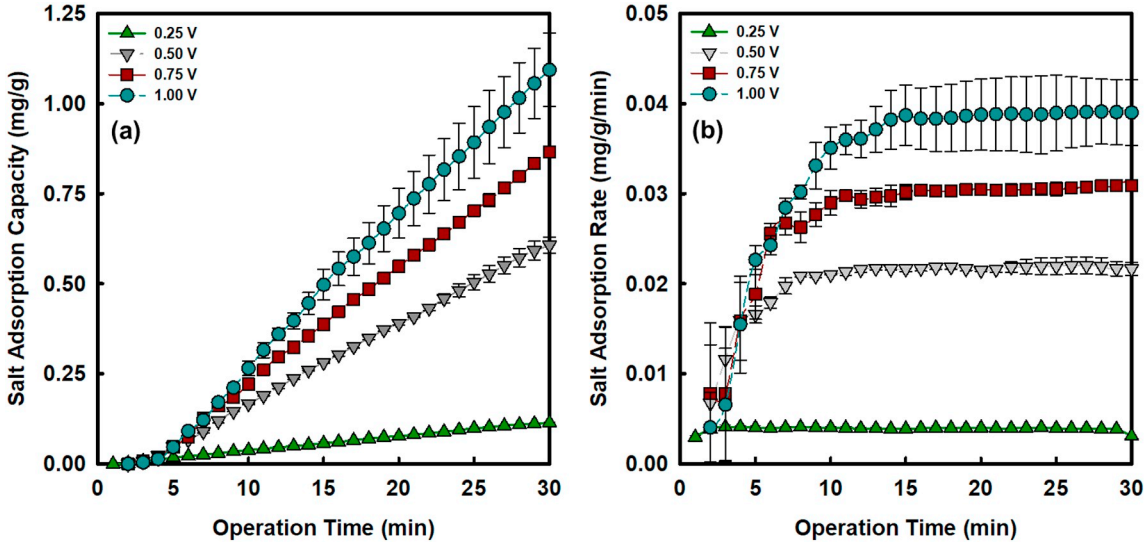

Fig. 8. FCDI standardized metrics with SWRO permeate feed water and seawater flow electrode in single mode: (a) salt adsorption capacity and (b) salt adsorption rate for 30-min operation on increasing the voltage in 0.25-V steps from 0.00 to 1.00 V.

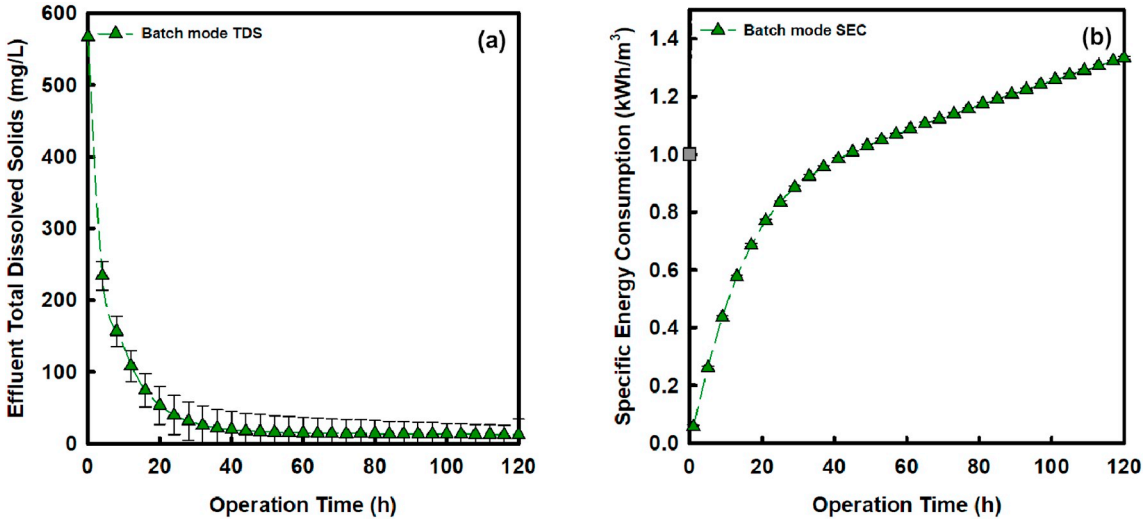

Fig. 9. FCDI performance with SWRO permeate feed water and seawater flow electrode in batch mode for 0.50 V with respect to (a) effluent total dissolved solids (mg/L) and (b) SEC (kWh/m^3) measured each hour.

installed, the FCDI can be more energy efficient than BWRO for obtaining the same water quality.

As shown in Fig. 10a, the SAC was calculated for 120-h batch-mode operation and reached a steady state after 30 h, achieving the maximum SAC (mSAC) of 0.26 mg/g. However, because FCDI uses a flow electrode, metrics other than the SAC should be considered because of the complexity of the cell components. We have assumed that the SAC results obtained from batch-mode operation simulate those of long-term single mode operation [41]. Furthermore, as shown in Fig. 10b, the ASAR was steady over the long-term operation, indicating a stable process. However, the ASAR of approximately 0.005 mg/(g min) was lower than that of single mode operation because of the differences in operation between single and batch modes [38].

In conclusion, the application of 0.50 V over long-term operation can yield a less concentrated effluent and a removal efficiency of > 95% was achieved with 120-h batch-mode operation, although the experimental conditions we selected would require further study, for example, the volume ratio of feed and electrolyte. Based on this result, the optimal conditions for scaling up the FCDI active area for obtaining the desired effluent concentration were determined. Thus, using our approach, the FCDI system can yield the target effluent concentration, which demonstrates the feasibility of the SWRO FCDI system.

4. Conclusions

Two-pass SWRO plants, which employ BWRO as the second pass, are frequently used in areas with highly saline feeds (e.g., the Middle East), and these plants suffer from high energy consumption issues. However, the energy requirements can be reduced by replacing the BWRO process with an electrochemical desalination process. Unlike the conventional MCDI process, FCDI is equipped with a flow electrode, which enables continuous operation with low energy consumption. In this study, we systematically investigated the feasibility of a SWRO-FCDI hybrid system using natural seawater in the flow electrode; this can be easily implemented in existing SWRO plants.

- The choice of a suitable electrolyte is crucial and strongly affects the performance of the SWRO-FCDI hybrid process. The use of the simulated seawater electrolyte (35,000 mg/L in TDS) resulted in more energy-efficient operation compared to the use of the simulated

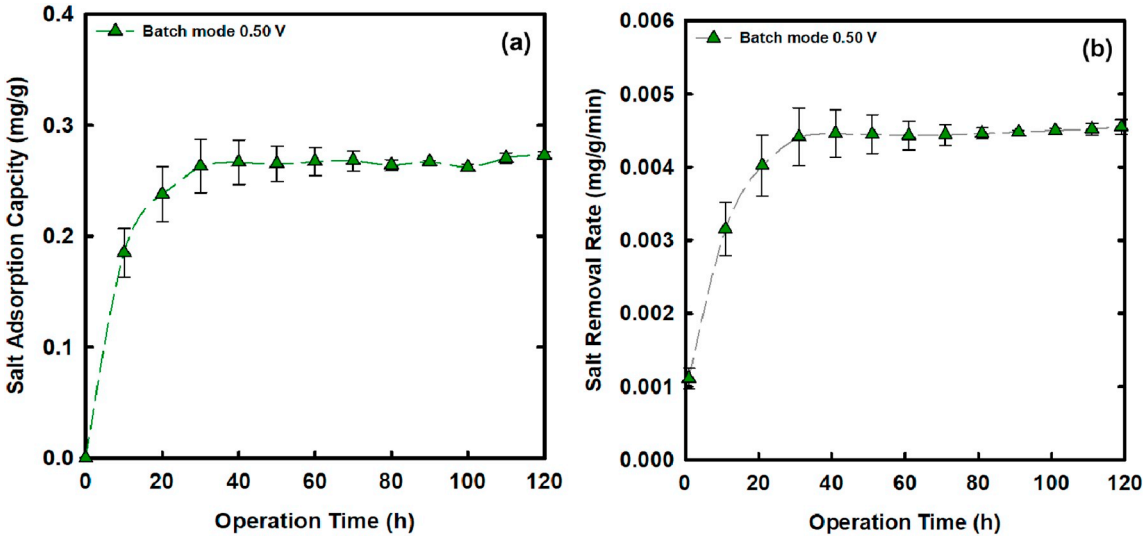

Fig. 10. Standardized metrics for FCDI with SWRO permeate feed water and seawater flow electrode in batch mode: (a) salt adsorption capacity and (b) salt adsorption rate over 120-h operation at 0.50 V.

SWRO concentrate, as well as resulting in increased removal efficiency.

- By employing a selective IEM, the FCDI was capable of selectively removing monovalent ions over divalent ions. Thus, water with a relatively higher divalent ion concentration than that produced by standard BWRO was produced; this is suitable for corrosion control in the subsequent pipe distribution systems.
- To investigate the feasibility of SWRO-FCDI system, actual SWRO permeate was treated in single mode with a real seawater electrolyte in the flow electrode. It was found that < 300 mg/L TDS can be obtained after 30-min operation at an HRT of 0.98 min.
- For optimization, the stability of long-term operation was examined in batch-mode operation, and > 95% removal efficiency and a SEC of 1.3 kWh/m^3 were achieved after 120 h in the batch mode. Furthermore, the calculation of the active FCDI area required to obtain the target water quality was possible.

Overall, the SWRO-FCDI hybrid system using a seawater flow electrode is energy efficient and can reduce the energetic burden of remineralization. By treating the SWRO permeate using the seawater flow electrode, water with satisfactory TDS levels was obtained. Further, the scaled-up active area of the SWRO-FCDI system required to obtain the target water quality can be calculated from lab-scale batch-mode operation. Having the benefits of low energy consumption and effective salt removal, the SWRO-FCDI system is promising for low-energy desalination.

CRediT authorship contribution statement

Hyun Jun Chung:Writing - original draft, Methodology, Visualization.**Jungbin Kim**:Conceptualization, Data curation, Writing - review & editing.**David Inhyuk Kim**:Conceptualization. **Gimun Gwak**:Visualization.**Seungkwan Hong**:Writing - review & editing, Funding acquisition, Supervision.

Declaration of competing interest

The authors declare that they have no known competing financial interests or personal relationships that could have appeared to influence the work reported in this paper.

Acknowledgment

This work was supported by Korea Environment Industry & Technology Institute (KEITI) through Industrial Facilities & Infrastructure Research Program, funded by Korea Ministry of Environment (MOE) (1485016424).

References

[1] J. Kim, K. Park, D.R. Yang, S. Hong, A comprehensive review of energy consumption of seawater reverse osmosis desalination plants, Appl. Energy 254 (2019) 113652.
[2] K. Park, J. Kim, D.R. Yang, S. Hong, Towards a low-energy seawater reverse osmosis desalination plant: a review and theoretical analysis for future directions, J. Membr. Sci. 595 (2020) 117607.
[3] B. Peñate, L. García-Rodríguez, Current trends and future prospects in the design of seawater reverse osmosis desalination technology, Desalination 284 (2012) 1–8.
[4] A.F. Ismail, M. Padaki, N. Hilal, T. Matsuura, W.J. Lau, Thin film composite membrane — Recent development and future potential, Desalination 356 (2015) 140–148.
[5] R.L. Stover, Seawater reverse osmosis with isobaric energy recovery devices, Desalination 203 (2007) 168–175.
[6] D.L. Shaffer, N.Y. Yip, J. Gilron, M. Elimelech, Seawater desalination for agriculture by integrated forward and reverse osmosis: improved product water quality for potentially less energy, J. Membr. Sci. 415–416 (2012) 1–8.
[7] J. Kim, S. Hong, A novel single-pass reverse osmosis configuration for high-purity water production and low energy consumption in seawater desalination, Desalination 429 (2018) 142–154.
[8] J. Kim, S. Hong, Optimizing seawater reverse osmosis with internally staged design to improve product water quality and energy efficiency, J. Membr. Sci. 568 (2018) 76–86.
[9] P. Dorji, J. Choi, D.I. Kim, S. Phuntsho, S. Hong, H.K. Shon, Membrane capacitive deionisation as an alternative to the 2nd pass for seawater reverse osmosis desalination plant for bromide removal, Desalination 433 (2018) 113–119.
[10] K. Dai, L. Shi, D. Zhang, J. Fang, NaCl adsorption in multi-walled carbon nanotube/active carbon combination electrode, Chem. Eng. Sci. 61 (2006) 428–433.
[11] Y.J. Kim, J.H. Choi, Improvement of desalination efficiency in capacitive deionization using a carbon electrode coated with an ion-exchange polymer, Water Res. 44 (2010) 990–996.
[12] J. Choi, Y. Oh, S. Chae, S. Hong, Membrane capacitive deionization-reverse electrodialysis hybrid system for improving energy efficiency of reverse osmosis seawater desalination, Desalination 462 (2019) 19–28.
[13] S.I. Jeon, H.R. Park, J.G. Yeo, S. Yang, C.H. Cho, M.H. Han, D.K. Kim, Desalination via a new membrane capacitive deionization process utilizing flow-electrodes, Energy Environ. Sci. 6 (2013) 1471–1475.
[14] J. Ma, D. He, W. Tang, P. Kovalsky, C. He, C. Zhang, T.D. Waite, Development of redox-active flow electrodes for high-performance capacitive deionization, Environ. Sci. Technol. 50 (2016) 13495–13501.
[15] H.R. Park, J. Choi, S. Yang, S.J. Kwak, S.I. Jeon, M.H. Han, D.K. Kim, Surface-modified spherical activated carbon for high carbon loading and its desalting performance in flow-electrode capacitive deionization, RSC Adv. 6 (2016) 69720–69727.
[16] G.J. Doornbusch, J.E. Dykstra, P.M. Biesheuvel, M.E. Suss, Fluidized bed electrodes with high carbon loading for water desalination by capacitive deionization, J. Mater. Chem. A 4 (2016) 3642–3647.
[17] P. Liang, X. Sun, Y. Bian, H. Zhang, X. Yang, Y. Jiang, P. Liu, X. Huang, Optimized desalination performance of high voltage flow-electrode capacitive deionization by adding carbon black in flow-electrode, Desalination 420 (2017) 63–69.
[18] S. Yang, H.R. Park, J. Yoo, H. Kim, J. Choi, M.H. Han, D.K. Kim, Plate-shaped graphite for improved performance of flow-electrode capacitive deionization, J. Electrochem. Soc. 164 (2017) E480–E488.
[19] K.B. Hatzell, M. Beidaghi, J.W. Campos, C.R. Dennison, E.C. Kumbur, Y. Gogotsi, A high performance pseudocapacitive suspension electrode for the electrochemical flow capacitor, Electrochim. Acta 111 (2013) 888–897.
[20] S. Yang, J. Choi, J.G. Yeo, S.I. Jeon, H.R. Park, D.K. Kim, Flow-electrode capacitive deionization using an aqueous electrolyte with a high salt concentration, Environ. Sci. Technol. 50 (2016) 5892–5899.
[21] C. Zhang, J. Ma, T.D. Waite, Ammonia-rich solution production from wastewaters using chemical-free flow-electrode capacitive deionization, ACS Sustain. Chem. Eng. 7 (2019) 6480–6485.
[22] A. Rommerskirchen, Y. Gendel, M. Wessling, Single module flow-electrode capacitive deionization for continuous water desalination, Electrochem. Commun. 60 (2015) 34–37.
[23] P. Nativ, O. Lahav, Y. Gendel, Separation of divalent and monovalent ions using flow-electrode capacitive deionization with nanofiltration membranes, Desalination 425 (2018) 123–129.
[24] S. Choi, B. Chang, J.H. Kang, M.S. Diallo, J.W. Choi, Energy-efficient hybrid FCDI-NF desalination process with tunable salt rejection and high water recovery, J. Membr. Sci. 541 (2017) 580–586.
[25] C. He, J. Ma, C. Zhang, J. Song, T.D. Waite, Short-circuited closed-cycle operation of flow-electrode CDI for brackish water softening, Environ. Sci. Technol. 52 (2018) 9350–9360.
[26] J. Liang, A. Deng, R. Xie, M. Gomez, J. Hu, J. Zhang, C.N. Ong, A. Adin, Impact of seawater reverse osmosis (SWRO) product remineralization on the corrosion rate of water distribution pipeline materials, Desalination 311 (2013) 54–61.
[27] D. Moreno, M.C. Hatzell, Influence of feed-electrode concentration differences in flow-electrode systems for capacitive deionization, Ind. Eng. Chem. Res. 57 (2018) 8802–8809.
[28] M.A. Brown, A. Goel, Z. Abbas, Effect of electrolyte concentration on the stern layer thickness at a charged interface, Angew. Chem. Int. Ed. 55 (2016) 3790–3794.
[29] R. Zhao, O. Satpradit, H.H.M. Rijnaarts, P.M. Biesheuvel, A. van der Wal, Optimization of salt adsorption rate in membrane capacitive deionization, Water Res. 47 (2013) 1941–1952.
[30] S.J. Duranceau, Desalination post-treatment considerations, Florida Water Resources Journal (2009) 4–18.
[31] A. Withers, Options for recarbonation, remineralisation and disinfection for desalination plants, Desalination 179 (2005) 11–24.
[32] J. Choi, H. Lee, S. Hong, Capacitive deionization (CDI) integrated with monovalent cation selective membrane for producing divalent cation-rich solution, Desalination 400 (2016) 38–46.
[33] B.B. Tanganov, About sizes of the hydrated salt ions–the components of sea water, European J. Nat. Hist. 1 (2013) 36–37.
[34] C.H. Hou, P. Taboada-Serrano, S. Yiacoumi, C. Tsouris, Electrosorption selectivity of ions from mixtures of electrolytes inside nanopores, J. Chem. Phys. 129 (2008) 224703.
[35] G.M. Geise, H.J. Cassady, D.R. Paul, B.E. Logan, M.A. Hickner, Specific ion effects on membrane potential and the permselectivity of ion exchange membranes, Phys. Chem. Chem. Phys. 16 (2014) 21673–21681.
[36] A. Zhu, P.D. Christofides, Y. Cohen, Minimization of energy consumption for a two-pass membrane desalination: effect of energy recovery, membrane rejection and retentate recycling, J. Membr. Sci. 339 (2009) 126–137.
[37] M.E. Suss, S. Porada, X. Sun, P.M. Biesheuvel, J. Yoon, V. Presser, Water desalination via capacitive deionization: what is it and what can we expect from it? Energy Environ. Sci. 8 (2015) 2296–2319.
[38] Y. Gendel, A.K.E. Rommerskirchen, O. David, M. Wessling, Batch mode and

continuous desalination of water using flowing carbon deionization (FCDI) technology, Electrochem. Commun. 46 (2014) 152–156.
[39] P. Nativ, Y. Badash, Y. Gendel, New insights into the mechanism of flow-electrode capacitive deionization, Electrochem. Commun. 76 (2017) 24–28.
[40] S. Porada, L. Weinstein, R. Dash, A. van der Wal, M. Bryjak, Y. Gogotsi, P.M. Biesheuvel, Water desalination using capacitive deionization with microporous carbon electrodes, ACS Appl. Mater. Interfaces 4 (2012) 1194–1199.
[41] S. Yang, H. Kim, S.-i. Jeon, J. Choi, J.-g. Yeo, H.-r. Park, J. Jin, D.K. Kim, Analysis of the desalting performance of flow-electrode capacitive deionization under short-circuited closed cycle operation, Desalination 424 (2017) 110–121.
[42] P. Zhang, J. Hu, W. Li, H. Qi, Research progress of brackish water desalination by reverse osmosis, J. Water Resource Prot. 5 (2013) 304.